UNIT-3

Corona Effects

3.1 Power Loss and Audible Noise

The average power-handling capacity of a 3-phase e.h.v. line and percentage loss due to I^2R heating were discussed. Representative values are given below for comparison purposes.

System kV	400		750		1000		1150	
Line Length, km	400	800	400	800	400	800	400	800
3-Phase MW/circuit ($P = 0.5\ V^2/xL$)	640	320	2860	1430	6000	3000	8640	4320
% Power Loss = 50 r/x	4.98%		2.4%		0.8%		0.6%	
kW/km Loss, 3-phase	80	20	170	42.5	120	30	130	32.5

When compared to the *I*2*R* heating loss, the average corona losses on several lines from 345 kV to 750 kV gave 1 to 20 kW/km in fair weather, the higher values referring to higher voltages. In foul-weather, the losses can go up to 300 kW/km. Since, however, rain does not fall all through the year (an average is 3 months of precipitation in any given locality) and precipitation does not cover the entire line length, the corona loss in kW/km cannot be compared to I^2R loss directly.

A reasonable estimate is the yearly average loss which amounts to roughly2 kW/km to 10 kW/km for 400 km lines, and 20-40 kW/km for 800 km range since usually higher voltages are necessary for the longer lines. Therefore, cumulative annual average corona loss amounts only to 10% of I^2R loss, on the assumption of continuous full load carried. With load factors of 60 to 70%, the corona loss will be a slightly higher percentage. Nonetheless, during rainy months, the generating station has to supply the heavy corona loss and in some cases it has been the experience that generating stations have been unable to supply full rated load to the transmission line. Thus, corona loss is a very serious aspect to be considered in line design.

When a line is energized and no corona is present, the current is a pure sine wave and capacitive. It leads the voltage by 90°, as shown in Figure 3.1(*a*). However, when corona is present, it calls for a loss component and a typical waveform of the total current is as shown in Figure 3.1 (*b*). When the two components are separated, the resulting inphase component has a waveform which is not purely sinusoidal, Figure 3.1 (*c*). It is still a current at power frequency, but only the fundamental component of this distorted current can result in power loss.

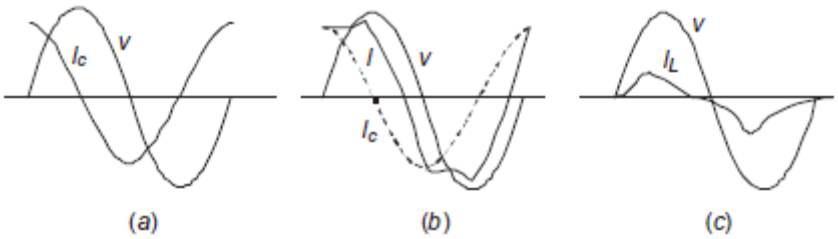

Fig. 3.1 Corona current waveform.

3.2 CORONA-LOSS FORMULAE

3.2.1 List of Formulae

Corona-loss formulae were initiated by F.W. Peek Jr. in 1911 derived empirically from most difficult and painstaking experimental work. Since then a horde of formulae have been derived by others, both from experiments and theoretical analysis. They all yield the power loss as a function of (*a*) the corona-inception voltage, *Vo*; (*b*) the actual voltage of conductor, *V*; (*c*) the excess voltage (*V* — *Vo*) above *Vo*; (*d*) conductor surface voltage gradient, *E*; (*e*) corona-inception gradient, *Eo*; (*f*) frequency, *f*; (*g*) conductor size, *d*, and number of conductors in bundle, *N*, as well as line configuration; (*h*) atmospheric condition, chiefly rate of rainfall, r, and (*i*) conductor surface condition.

A. Those Based on Voltages

(i) Linear relationship : Skilling's formula (1931):

$$Pc \; \alpha \; V - Vo$$

(*ii*) *Quadratic relationship*

(*a*) Peek's formula (1911):

$$Pc \; \alpha \; (V - Vo)^2$$

(*b*) Ryan and Henline formula (1924):

$$Pc \; \alpha \; V \, (V - Vo)$$

(*c*) Peterson's formula (1933) :

$$Pc \; \alpha \; V^2 . \, F \, (V/Vo)$$

where *F* is an experimental factor.

(*iii*) *Cubic Relationship*

(*a*) Foust and Menger formula (1928):

$$Pc \; \alpha \; V^3$$

(*b*) Prinz's formula (1940):

$$Pc \alpha V^2 (V - V_o)$$

B. Those Based on Voltage Gradients

(*a*) Nigol and Cassan formula (1961):

$$Pc \alpha E2 \text{ In } (E/E_o)$$

(*b*) Project *EHV* formula (1966):

$$Pc \alpha V.Em, \text{ m} = 5$$

In order to obtain corona-loss figures from e.h.v. conductor configurations, outdoor experimental projects are established in countries where such lines will be strung. The resulting measured values pertain to individual cases which depend on local climatic conditions existing at the projects. It is therefore difficult to make a general statement concerning which formula or loss figures fit coronal losses universally.

3.3 CHARGE-VOLTAGE (*q – V*) DIAGRAM AND CORONA LOSS

3.3.1 Increase in Effective Radius of Conductor and Coupling Factors

The partial discharge of air around a line conductor is the process of creation and movement of charged particles and ions in the vicinity of a conductor under the applied voltage and field. We shall consider a simplified picture for conditions occurring when first the voltage is passing through the negative half-cycle and next the positive half-cycle, as shown in Figure 3.2.

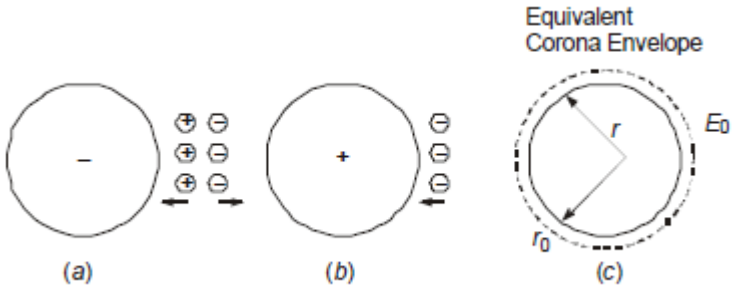

Fig. 3.2 Space-charge distribution in corona and increase in effective radius of conductor

In Figure 3.2(*a*), free electrons near the negative conductor when repelled can acquire sufficient energy to form an electron avalanche. The positive ions (a neutral molecule which has lost an electron) are attracted towards the negative conductor while the electrons drift into lower fields to attach themselves to neutral atoms or molecules of Nitrogen and Oxygen to form negative ions. Some recombination could also take place. The energy imparted for causing initial

ionization by collision is supplied by the electric field. During the positive half cycle, the negative ions are attracted towards the conductor, but because of local conditions not all ions drift back to the conductor. A space charge is left behind and the hysteresis effect gives rise to the energy loss. Furthermore, because of the presence of charged particles, the effective charge of the conductor ground electrode system is increased giving rise to an increase in effective capacitance. This can be interpreted in an alternative manner by assuming that the conductor diameter is effectively increased by the conducting channel up to a certain extent where the electric field intensity decreases to a value equal to that required for further ionization, namely, the corona-inception gradient, Figure 3.2(*c*).

3.4 AUDIBLE NOISE: GENERATION AND CHARACTERISTICS

When corona is present on the conductors, e.h.v. lines generate audible noise which is especially high during foul weather. The noise is broadband, which extends from very low frequency to about 20 kHz. Corona discharges generate positive and negative ions which are alternately attracted and repelled by the periodic reversal of polarity of the ac excitation. Their movement gives rise to sound-pressure waves at frequencies of twice the power frequency and its multiples, in addition to the broadband spectrum which is the result of random motions of the ions, as shown in Figure 3.3. The noise has a pure tone superimposed on the broadband noise. Due to differences in ionic motion between ac and dc excitations, dc lines exhibit only a broad bandnoise, and furthermore, unlike for ac lines, the noise generated from a dc line is nearly equal in both fair and foul weather conditions. Since audible noise (AN) is man-made, it is measured in the same manner as other types of man-made noise such as aircraft noise, automobile ignition noise, transformer hum, etc.

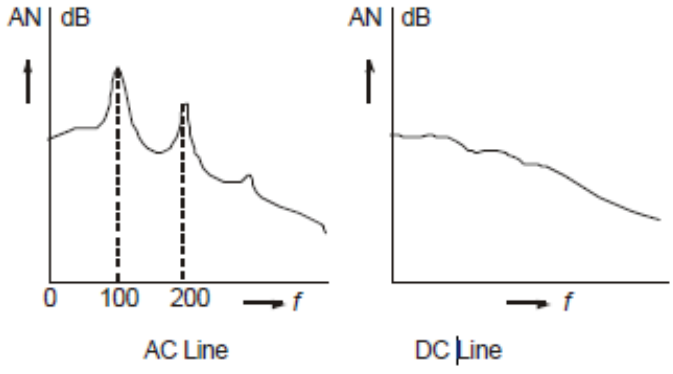

Fig. 3.3 Audible Noise frequency spectra from ac and dc transmission lines.

Audible noise can become a serious problem from 'psycho-acoustics' point of view, leading to insanity due to loss of sleep at night to inhabitants residing close to an e.h.v. line. This problem came into focus in the 1960's with the energization of 500 kV lines in the USA. Regulatory bodies have not as yet fixed limits to AN from power transmission lines since such regulations do not exist for other man-made sources of noise. The problem is left as a social one which has to be settled by public opinion.

3.5 LIMITS FOR AUDIBLE NOISE

Since no legislation exists setting limits for AN for man-made sources, power companies and environmentalists have fixed limits from public-relations point of view which power companies have accepted from a moral point of view. In doing so, like other kinds of interference, human beings must be subjected to listening tests. Such objective tests are performed by every civic minded power utility organization. The first such series of tests performed from a 500-kV line of the Bonneville Power Administration in the U.S.A. is known as Perry Criterion. The AN limits are as follows:

No complaints : Less than 52.5 dB (*A*),

Few complaints : 52.5 dB (A) to 59 dB (*A*),

Many complaints : Greater than 59 dB (*A*),

The reference level for audible noise and the dB relation will be explained later. The notation (*A*) denotes that the noise is measured on a meter on a filter designated as *A*-weighting network. There are several such networks in a meter.

Design of line dimensions at e.h.v. levels is now governed more by the need to limit AN levels to the above values. The selection of width of line corridor or right-of-way (R-O-W), where the nearest house can be permitted to be located, if fixed from AN limit of 52.5 dB(*A*),

will be found adequate from other points of view at 1000 to 1200 kV levels. The audible noise generated by a line is a function of the following factors:

(a) the surface voltage gradient on conductors,

(*b*) the number of sub-conductors in the bundle,

(*c*) conductor diameter,

(d) atmospheric conditions, and

(*e*) the lateral distance (or aerial distance) from the line conductors to the point where noise is to be evaluated.

The entire phenomenon is statistical in nature, as in all problems related to e.h.v. line designs, because of atmospheric conditions. with atmospheric conditions but also with the hours of the day and night during a 24-hour period. The reason is that a certain noise level which can be tolerated during the waking hours of the day,

when ambient noise is high, cannot be tolerated during sleeping hours of the night when little or no ambient noises are present.

3.6 CORONA PULSES: THEIR GENERATION AND PROPERTIES

There are in general two types of corona discharge from transmission-line conductors: (i) Pulse less or Glow Corona; (ii) Pulse Type or Streamer Corona. Both these give rise to energy loss, but only the pulse-type of corona gives interference to radio broadcast in the range of 0.5 MHz to 1.6 MHz. In addition to corona generated on line conductors, there are spark discharges from chipped or broken insulators and loose guy wires which interfere with TV reception in the 80–200 MHz range.

Corona on conductors also causes interference to Carrier Communication and Signalling in the frequency range 30 kHz to 500 kHz. In the case of Radio and TV interference the problem is one of locating the receivers far enough from the line in a lateral direction such that noise generated by the line is low enough at the receiver location in order to yield a satisfactory quality of reception. In the case of carrier interference, the problem is one of determining the transmitter and receiver powers to combat line-generated noise power. In the case of Radio and TV interference the problem is one of locating the receivers far enough from the line in a lateral direction such that noise generated by the line is low enough at the receiver location in order to yield a satisfactory quality of reception. In the case of carrier interference, the problem is one of determining the transmitter and receiver powers to combat line-generated noise power.

As in most gas discharge phenomena under high impressed electric fields, free electrons and charged particles (ions) are created in space which contains very few initial electrons. We can therefore expect a build up of resulting current in the conductor from a zero value to a maximum or peak caused by the avalanche mechanism and their motion towards the proper electrode. Once the peak value is reached there is a fall in current because of lowering of electric field due to the relatively heavy immobile space charge cloud which lowers the velocity of ions. We can therefore expect pulses to be generated with short crest times and relatively longer fall times. Measurements made of single pulses by the author in co-axial cylindrical arrangement are shown in Figure 3.4 under dc excitation. Similar pulses occur during the positive and negative half-cycles under ac excitation. The best equations that fit the observed wave shapes are also given on the figures. It will be assumed that positive corona pulses have the equation

$$i_+ = k_+ i_p (e^{-\alpha t} - e^{-\beta t})$$

while negative pulses can be best described by

$$i_- = k_- i_p t^{-3/2} . e^{-\gamma/t - \delta t}$$

These equations have formed the basis for calculating the response of bandwidth-limited radio receivers (noise meters), and for formulating mathematical models of the radio-noise problem.

In addition to the wave shape of a single pulse, their repetition rate in a train of pulses is also important.

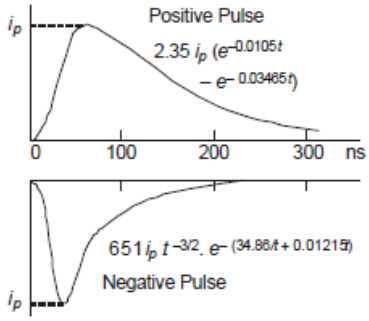

Fig. 3.4 Single positive and negative pulses

$$i_+ = k_+ i_p (e^{-\alpha t} - e^{-\beta t});\ i_- = k_- i_p . t^{-1.5} . e^{(-\gamma/t - \delta t)}$$

Referring to Fig. 6.2, when a conductor is positive with respect to ground, an electron avalanche moves rapidly into the conductor leaving the heavy positive-ion charge cloud close to the conductor which drifts away. The rapid movement of electrons and motion of positive-ions gives the steep front of the pulse, while the further drift of the positive-ion cloud will form the tail of the pulse. It is clear that the presence of positive charges near the positive conductor lowers the field to an extent that the induced current in the conductor nearly vanishes. As soon as the positive-ions have drifted far enough due to wind or neutralized by other agencies such as free electrons by recombination, the electric field in the vicinity of the conductor regains sufficiently high value for pulse formation to repeat itself. Thus, a train of pulses results from a point in corona on the conductor. The repetition rate of pulses is governed by factors local to the conductor. It has been observed that only one pulse usually occurs during a positive half cycle in fair weather and could increase to about 10 in rain where the water sprays resulting from breaking raindrops under the applied field control electrical conditions local to the conductor.

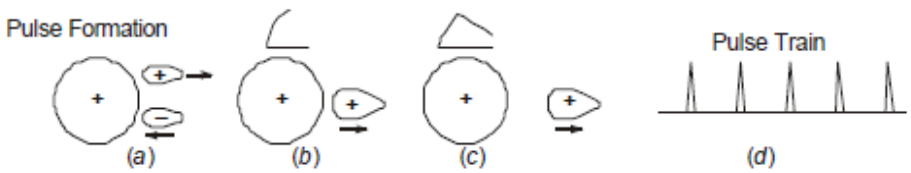

Fig. 3.4 Formation of pulse train from positive polarity conductor.

The situation when the conductor is negative with respect to ground is the reverse of that described above. The electron avalanche moves away from the conductor while the positive-ion cloud moves towards the negatively-charged conductor. However, since the heavy positive-ions are moving into progressively higher electric fields, their motion is very rapid which gives rise to a much sharper pulse than a positive pulse. Similarly, the lighter electrons move rapidly away from the conductor and the electric field near the conductor regains its original value for the next pulse generation quicker than for the positive case. Therefore, negative pulses are smaller in amplitude, have much smaller rise and fall times but much higher repetition rates than positive pulses. It must at once be evident that all the properties of positive and negative pulses are random in nature and can only be described through random variables.

Typical average values of pulse properties are as follows:

Type	*Time to Crest*	*Time to 50% on Tail*	*Peak Value of Current*	*Repetition Rate Pulses per Second*	
				A.C.	*D.C.*
Positive	50 ns	200 ns	100 mA	Power Freq.	1,000
Negative	20 ns	50 ns	10 mA	100 × P.F.	10,000

Pulses are larger as the diameter of conductor increases because the reduction in electric field strength as one moves away from the conductor is not as steep as for a smaller conductor so that conditions for longer pulse duration are more favorable. In very small wires, positive pulses can be absent and only a glow corona can result, although negative pulses are present when they are known as Trichel Pulses named after the first discoverer of the pulse-type discharge. Therefore, only positive polarity pulses are important because of their larger amplitudes even though their repetition rate is lower than negative pulses.

3.7 FREQUENCY SPECTRUM OF THE RI FIELD OF LINE

The frequency spectrum of radio noise refers to the variation of noise level in μV or μV/m (or their dB values referred to 1 μV or 1μV/m) with frequency of measurement.

$$A(w) = K i_p . (\beta - \alpha) / \sqrt{(\alpha^2 + w^2)(\beta^2 + w^2)}$$

On a long line, there exist a very large number of points in corona and a noise meter located in the vicinity of the line (usually at or near ground level) responds to a train of pulses originating from them. The width of a single pulse is about 200 ns (0.2 □s) while the separation of pulses as seen by the input end of the meter could be 1 □s or more. Therefore, it is unusual for positive pulses to overlap and

the noise is considered as impulsive. When pulses overlap, the noise is random. Measurements indicate that from a long line, the RI frequency spectrum follows closely.

$$RI(w) \propto f^{-1} \text{ to } f^{-1.5}$$

Thus, at 0.5 MHz the noise is 6-9 dB higher than at 1 MHz, while at 2 MHz it is 6–9 dB lower. In practice, these are the adders suggested to convert measured noise at any frequency to 1 MHz level. The frequency spectrum is therefore very important in order to convert noise levels measured at one frequency to another. This happens when powerful station signal interferes with noise measurements from a line so that measurements have to be carried out at a frequency at which no broadcast station is radiating.

The frequency spectrum from corona generated line noise is nearly fixed in its characteristic so that any deviation from it as measured on a noise meter is an indication of sources other than the line, which is termed "back ground noise". In case a strong source of noise is present nearby, which is usually a factory with motors that are sparking or a broken insulator on the tower, this can be easily recognized since these usually yield high noise levels up to 30 MHz and their frequency spectrum is relatively flat.

3.8 LATERAL PROFILE OF RI AND MODES OF PROPAGATION

The most important aspect of line design from interference point of view is the choice of conductor size, number of sub-conductors in bundle, line height, and phase spacing. Next in importance is the fixing of the width of line corridor for purchase of land for the right-of-way. The lateral decrement of radio noise measured at ground level as one moves away from the line has the profile sketched in Fig. 3.5. It exhibits a characteristic double hump within the space between the conductors and then decreases monotonically as the meter is moved away from the outer phase.

Receiver should be located within the distance d_0 from the outer phase or dc from the line centre. Therefore, it becomes essential to measure or to be able to calculate at design stages the lateral profile very accurately from a proposed line in order to advise regulatory bodies on the location of receivers. In practice, many complaints are heard from the public who experience interference to radio broadcasts if the line is located too close to their homesteads when the power company routes an e.h.v. line wrongly. In such cases, it is the engineer's duty to recommend remedies and at times appear as witness in judicial courts to testify on the facts of a case.

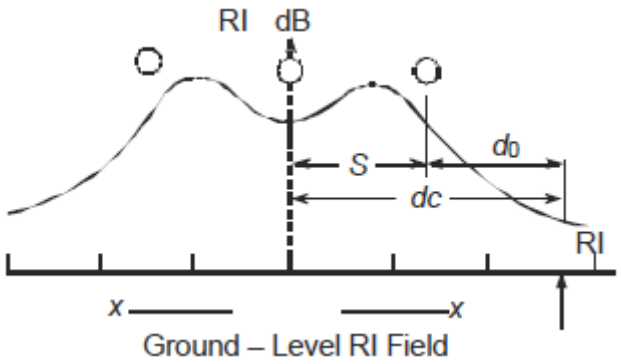

Fig. 3.5 Lateral profile of RI at ground level for fixing width of right-of-way of line

for the radio-frequency energy on the multi-conductor line. This is the basis for determining the expected noise profile from a chosen conductor size and line configuration in un-transposed and fully-transposed condition. We consider 6 preliminary cases of charge distribution on the line conductors after which we will combine these suitably for evaluating the total noise level of a line. In all these cases, the problem is to calculate the field strength at the location of a noise meter when the *r-f* charge distribution is known.

Here, we consider the vertical component of ground-level field intensity which can be related to the horizontal component of magnetic field intensity by the characteristic impedance of free space. We restrict our attention to horizontal 3-phase line for the present. In every case, only the magnitude is of concern.

3. 9 The RI Excitation Function

With the advent of voltages higher than 750 kV, the number of sub conductors used in a bundle has become more than 4 so that the CIGRE formula does not apply. Moreover, very little experience of RI levels of 750 kV lines were available when the CIGRE formula was evolved, as compared to the vast experience with lines for 230 kV, 345 kV, 400 kV and 500 kV. Several attempts were made since the 1950's to evolve a rational method for predicting the RI level of a line at the design stages before it is actually built when all the important line parameters are varied. These are the conductor diameter, number of sub-conductors, bundle spacing or bundle radius, phase spacing, line height, line configuration (horizontal or delta), and the weather variables. The most important concept resulting from such an attempt in recent years is the "Excitation Function" or the "Generating Function" of corona current injected at a given radio frequency in unit bandwidth into the conductor. This quantity is determined experimentally from measurements

carried out with short lengths of conductor strung inside a cylindrical or rectangular cage.

Consider Fig. 3.6 which shows a source of corona at *S* located at a distance *x* from one end of a line of length *L*. According to the method using the Excitation Function to predict the RI level with given dimensions and conductor geometry, the corona source at *S* on the conductor generates an excitation function *I* measured in mA/ m. The line has a surge impedance *Z*0 so that r-f power generated per unit length of line is

$$E = I^2 Z_0$$

$E = I^2 Z_0$

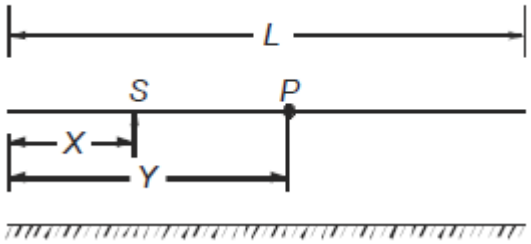

Fig. 3.6 The excitation function and its propagation on line for RI calculation.

Under rain, a uniform energy or power per unit bandwidth is generated so that in a differentiallength *dx*, the power generated is (*E.dx*). In this method, we calculate the RI level under rain first and deduct 17 dB to obtain fair-weather RI. This power will split equally in two directions and travel along the line to reach the point *P* at a distance (*y*–*x*) from the source *S*. In doing so, it will attenuate to the value $e^{-2a(y-x)}$, where a = attenuation factor for voltage in Nepers per unit length. Therefore, the total energy received at *P* due to all sources to the left of *P* will be

$$E_L = \int_0^y \frac{1}{2}(E.dx).e^{-2a(y-x)} = \frac{E}{4a}(1 - e^{-2ay})$$

Similarly, the energy received at *P* due to all sources to its right will be

$$E_R = \frac{E}{4a}(1 - e^{-2a(L-y)})$$

For a line of finite length, repeated reflections occur from the ends, but for a very long line these are not of consequence. Also, unless the point *P* is located very close to the ends, the exponential terms can be neglected. Therefore, the total r-f energy received at *P* will be

$$Ep = E/2a$$

which shows that all points on a long line receive the same r-f energy when the corona generation is uniform.

3.10 MEASUREMENT OF RI, RIV, AND EXCITATION FUNCTION

The interference to AM broadcast in the frequency range 0.5 MHz to 1.6 MHz is measured in terms of the three quantities : Radio Interference Field Intensity (RIFI or RI), the Radio Influence Voltage (RIV), and more recently through the Excitation Function. Their units are mV/m, mV, and mA/ m or the decibel values above their reference values of 1 unit (mV /m, mV,mA / m). The nuisance value for radio reception is governed by a quantity or level which is nearly equal to the peak value of the quantity and termed the Quasi Peak. A block diagram of a radio noise meter is shown in Fig. 3.7. The input to the meter is at radio frequency (r-f) which is amplified and fed to a mixer.

The rest of the circuit works exactly the same as a highly sensitive super heterodyne radio receiver, However, at the IF output stage, a filter with 5 kHz or 9 kHz bandwidth is present whose output is detected by the diode *D*. Its output charges a capacitance *C* through a low resistance *Rc* such that the charging time constant $Tc = Rc\ C = 1$ ms. A second resistance *Rd* is in parallel with *C* which is arranged to give a time constant $Td = Rd\ C = 600$ ms in ANSI meters and 160 ms in CISPR or European standard meters. Field tests have shown that there is not considerable difference in the output when comparing both time constants for line-generated corona noise. The voltage across the capacitor can either be read as a current through the discharge resistor *Rd* or a micro-voltmeter connected across it.

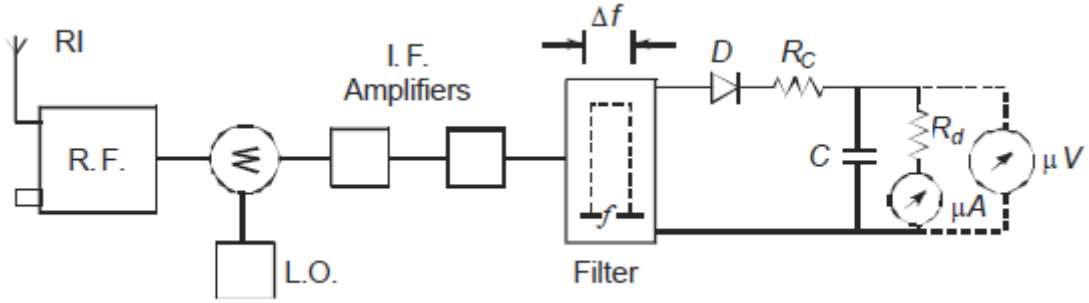

Fig. 3.7 Block diagram of Radio Noise Meter.

3.11 MEASUREMENT OF EXCITATION FUNCTION

The corona generating function or the excitation function caused by injected current at radio frequencies from a corona discharge is measured on short lengths of conductor strung inside "cages"

Some examples of measuring radio noise and injected current are shown in Fig. 3.8. In every case the measured quantity is RIV at a fixed frequency and the excitation function calculated. filter provides an attenuation of at least 25 dB so that the RI current is solely due to corona on conductor. The conductor is

terminated in a capacitance *Cc* at one end in series with resistances *R*1 and *Rc*, while the other end is left open. The conductor is strung with strain insulator at both ends which can be considered to offer a very high impedance at 1MHz so that there is an open-termination. But this must be checked experimentally in situ. The coupling capacitor has negligible reactance at r-f so that the termination at the measuring end is nearly equal to (*R*1 + *Rc*), where *Rc* = surge impedance of the cable to the noise meter. The resistance *Rc* is also equal to the input impedance of the noise meter.

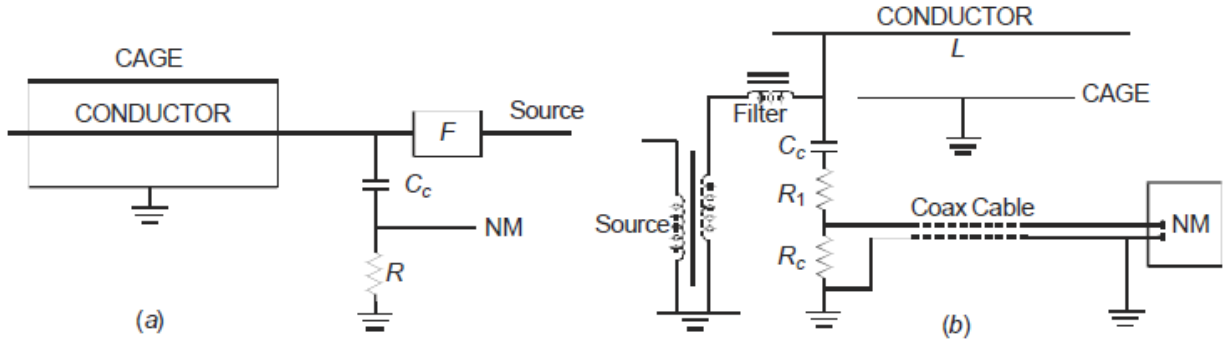

Fig. 3.8 Cage setups for measuring excitation function with measuring circuit.